A Multi-Model approach to evaluating target phosphorus loads for Lake Erie

Donald Scavia[1,*], Joseph V. DePinto[2], Isabella Bertani[1]

[1] Water Center, Graham Sustainability Institute, University of Michigan, 625 East Liberty Road, Ann Arbor, MI 48193, USA

[2] LimnoTech, 501 Avis Drive, Ann Arbor, MI 48108, USA

* Corresponding author: scavia@umich.edu

ABSTRACT

In response to water quality changes in the Great Lakes since implementing the 1978 Amendment to the Great Lakes Water Quality Agreement, the US and Canada renegotiated the agreement in 2012, requiring the governments to review and revise phosphorus (P) load targets, starting with Lake Erie. In response, the governments supported a multi-model team to evaluate the existing objectives and P load targets for Lake Erie and provide the information needed to update those targets. Herein, we describe the process and resulting advice provided to the binational process. The collective modeling effort concluded that avoiding severe Western Basin (WB) cyanobacteria blooms requires a focus on reducing total P loading from the Maumee River, with an emphasis on high-flow events during March – July, that focusing on the dissolved reactive P load alone will not be sufficient, and that load from the Detroit River is not a driver of cyanobacteria blooms. Reducing Central Basin (CB) hypoxia requires a CB+WB load reduction greater than what is needed to reach the WB cyanobacteria biomass goal. The whole lake load for achieving a *Cladophora* threshold is higher than that required for the hypoxia and cyanobacteria thresholds. In general, the loads needed to meet assumed thresholds were roughly 40% of the 2008 loads.

Keywords: Loading targets, Great Lakes Water Quality Agreement, Lake Erie, Eutrophication Models

32

Introduction

In response to significant water quality changes in the Great Lakes since implementing the 1978 Amendment to the Great Lakes Water Quality Agreement (GLWQA) (e.g., Evans et al., 2011; IJC, 2014; Scavia et al., 2014), the US and Canada renegotiated the GLWQA (GLWQA, 2012). Annex 4 of the 2012 GLWQA Protocol set interim phosphorus (P) loading targets identical to those established in the 1978 Amendment, and required the US and Canadian governments to review those targets and recommend adjustments if needed, starting with Lake Erie.

As part of the GLWQA review, a committee of modelers examined data and models used to support the P target loads in the 1978 Amendment relative to the current status of the Lakes and models (DePinto et al., 2006). At that time, a set of Great Lakes eutrophication models were used to help establish target P loads designed to eliminate excess algae growth and to reduce areas of low dissolved oxygen (DO) concentration – key eutrophication symptoms at that time. Those models ranged from simple empirical relationships to kinetically complex, process-oriented models (Bierman, 1980; Vallentyne and Thomas, 1978), and post-audit of several of those models confirmed they had established sound relationships between P loading and system-wide averaged P and chlorophyll-*a* concentrations (e.g., DiToro et al., 1987; Lesht et al., 1991).

However, DePinto et al. (2006) concluded that those models were not spatially resolved enough to capture the characteristics of nearshore eutrophication, nor the impacts of more recent ecosystem changes, such as impacts from dreissenid mussels and other invasive species. Nor were they designed to address harmful algal blooms (HABs). Their recommendation was to establish a new effort to quantify relative contributions of the factors controlling Great Lakes re-eutrophication (Scavia et al., 2014), and to revise quantitative relationships among those stressors and eutrophication indicators such as HABs, hypoxia, and nuisance benthic algae.

In response, several new Great Lakes modeling efforts were initiated, and given the availability of these new models, the Parties supported a new team to evaluate the interim P objectives and load targets for Lake Erie and provide the information needed to update those targets. Herein, we describe that process and the resulting advice provided to the GLWQA process because the Lake Erie plan was intended to also serve as a template for the other Great Lakes.

Approach

Ecosystem Response Indicators – Before initiating the modeling work, Ecosystem Response Indicators (ERIs) and their associated metrics were established with the Annex 4 Nutrient Objectives and Targets Task Team (GLWQA, 2015). Four ERIs of Lake Erie eutrophication were selected:

- *Western Basin (WB) cyanobacteria biomass* represented by the maximum 30-day average cyanobacteria biomass
- *Central Basin (CB) hypoxia* represented by number of hypoxic days; average extent of hypoxic area during summer; and average hypolimnion DO concentration during August and September
- *Basin-specific overall phytoplankton biomass* represented by summer average chlorophyll-*a* concentration
- *Eastern Basin (EB) Cladophora* represented by dry weight biomass and stored P content.

Multi-Model Strategy – A multi-model approach was used to explore relationships between the ERIs and P loads because a suite of models with a broad range of complexities and approaches affords an informative comparison of results. Bierman and Scavia (2013) and Weller et al. (2013) identified a number of benefits of applying multiple models of differing complexity:

- Problems and data are viewed from different conceptual and operational perspectives
- The level of risk in environmental management decisions is reduced
- Model diversity adds more value to the decision process than model multiplicity
- Findings are stronger when multiple lines of evidence are available
- Using multiple models increases knowledge and understanding of underlying processes
- Average predictions from a set of models are typically better than from a single model
- Information from multiple models can help quantify uncertainty
- Multiple models can expand opportunities for additional stakeholders to participate
- Reconciling differences among models provides insights on key sources and processes

There is also precedent for using multi-model approaches to support management decisions. As noted above, this approach was used in the late 1970's to establish the original target P loads for the Great Lakes (Bierman, 1980). In that case, the six models ranged in complexity from an empirical steady state model (Vollenweider, 1976) to more complex, mechanistic models of Lake Erie (Di Toro and Connolly, 1980) and Saginaw Bay (Bierman and Dolan, 1981). Additional examples include addressing polychlorinated biphenyls (PCBs) in Lake Ontario (IJC, 1988), and nutrient loads for the Neuse River Estuary (Stow et al., 2003), the Gulf of Mexico (Scavia et al., 2004), and the Chesapeake Bay (Weller et al., 2013).

After establishing the ERIs, model equations, coefficients, driving variables, assumptions, and time step of predictions were described; calibrations, confirmations, and uncertainties/sensitivities were compared; and the ability of each model to develop ERI metric load-response curves were reviewed. With this information and results from previous

publications, the model capabilities were reviewed with respect to the following evaluation criteria:

- *Applicability to ERI metrics:* The models' ability to address the spatial, temporal, and kinetic characteristics of the ERI metrics. While models that address other objectives can be informative, highest priority was given to those that can address the ERIs directly.
- *Extent/quality of calibration and confirmation:* *Calibration* – The models' ability to reproduce ERI metric state-variables and internal processes. *Post-calibration testing* – The models' ability to replicate conditions not represented in the calibration data set.
- *Extent of model documentation:* The extent of documentation, including descriptions of model kinetics calculations, inputs, calibration, confirmation, and applications.
- *Level of uncertainty analysis:* The extent to which the models evaluated uncertainty and sensitivity, including for example, those associated with measurement error, model structure, parameterization, aggregation, and uncertainty in characterizing natural variability.

The Models - The models that satisfied these criteria are summarized in Table 1 and described briefly below. Model formulation, calibration, confirmation, and sensitivity/uncertainty, as well as the construction of load-response curves are provided in more detail in Scavia and DePinto (2015), in the series of papers published in this issue (Bertani et al., this issue; Bocaniov et al., this issue; Chapra et al., this issue; Rucinski et al., this issue; Stumpf et al., this issue; Verhamme et al., this issue; Zhang et al., this issue), in Auer et al. (2010), Canale and Auer (1982), Tomlinson et al. (2010) and in Lam et al. (2008, 1987, 1983).

120 *Total Phosphorus Mass Balance Model* (Chapra et al., this issue) – The original version of this
121 parsimonious total phosphorus (TP) mass balance model was used (along with other models) to
122 establish P loading targets for the 1978 Great Lakes Water Quality Agreement. The model has
123 been subsequently revised and updated, including the expansion of the calibration dataset
124 through 2010 and an increase in the post-1990 apparent TP settling velocity to improve model
125 performance, suggesting that mussel invasion may have enhanced the lakes' ability to retain P
126 (Chapra and Dolan, 2012). The model predicts annual average TP concentrations in the offshore
127 waters of the Great Lakes as a function of external load. For Lake Erie, the model computes
128 basin-wide annual average TP concentrations as a function of loads to each basin. In this
129 application, an empirical relationship between summer chlorophyll and TP concentrations
130 derived for each basin was used to predict basin-specific average chlorophyll levels under
131 different TP load scenarios.

132 *U-M/GLERL Western Lake Erie HAB Model* (Bertani et al., this issue) – A probabilistic
133 empirical model developed by Obenour et al. (2014) relates peak summer cyanobacteria biomass
134 in the WB to spring P loading from the Maumee River. The model is calibrated to multiple sets
135 of *in situ* and remotely sensed bloom observations through a Bayesian hierarchical approach that
136 allows for rigorous uncertainty quantification. The model includes a temporal trend component
137 that suggests an apparent increased susceptibility to cyanobacteria blooms over time. For this
138 application, the original model (Obenour et al., 2014) was modified to include an empirical
139 estimate of the bioavailable portion of the TP load as bloom predictor.

140 *NOAA Western Lake Erie HAB Model* (Stumpf et al., this issue) - This model is based on an
141 empirical regression between spring P load or flow from the Maumee River and peak summer
142 cyanobacteria biomass in the WB as determined through satellite imagery (Stumpf et al., 2012).

143 For this application, the model has been modified to account for the potential difference in
144 cyanobacteria response to load intensity in warm vs. relatively cold early summers. An estimate
145 of bioavailable P load was also tested as bloom predictor.

146 *Nine-Box Model* (Lam et al., 2008, 1987, 1983) - This coarse grid (9-box) P mass balance model
147 was developed to quantify the main physical and biochemical processes that influence Lake Erie
148 eutrophication and related hypoxia (Lam et al., 1983). The model was previously calibrated and
149 validated with water quality observations from 1967-1982 (Lam et al., 1987). For this
150 application, the original calibration was modified to account for changes in settling and re-
151 suspension processes due to dreissenid mussel invasion (see Scavia and DePinto, 2015).

152 *1-Dimensional Central Basin Hypoxia Model* (Rucinski et al., this issue) - A one-dimensional
153 linked vertical hydrodynamic and eutrophication model was previously developed, calibrated,
154 and corroborated with water quality observations in the CB (Rucinski et al., 2014, 2010). The
155 model is driven by a 1-D hydrodynamic model that provides temperature and vertical mixing
156 profiles. The biological portion of the model incorporates P and carbon (C) loading and internal
157 cycling, algal growth and decay, zooplankton grazing, water column oxygen consumption and
158 production processes, and sediment oxygen demand (SOD). The model has been tested with 19
159 years (1987-2005) of observed loading rates and meteorological conditions to understand the
160 relative contribution of stratification conditions versus P loading extent and seasonal timing on
161 the severity of hypoxia in the CB.

162 *Ecological Model of Lake Erie - EcoLE* (Zhang et al., this issue) - A two-dimensional
163 hydrodynamic and water quality model based on the CE-QUAL-W2 framework was developed
164 and applied to Lake Erie (Zhang et al., 2008). The model was calibrated with observations from
165 1997 and verified with data collected in 1998 and 1999. The model has been used to estimate

the impact of grazing and nutrient excretion by dreissenid mussels on phytoplankton biomass and seasonal succession (Zhang et al., 2011). As part of this application, the model was also used to estimate the spatial distribution and relative contribution of different external and internal P sources to the overall P lake budget.

Western Lake Erie Ecosystem Model - WLEEM (Verhamme et al., this issue) - The Western Lake Erie Ecosystem Model (WLEEM) is a three-dimensional, fine-scale, process-based, linked hydrodynamic-sediment transport-eutrophication model developed to simulate water quality responses to changes in meteorological conditions and loads of water, sediments, and nutrients to the WB. The numerous state variables encompass three phytoplankton groups, including cyanobacteria. In this application the model was used to simulate the response of WB summer cyanobacteria biomass to a broad suite of P load scenarios, including assessing the impact of potential load reduction strategies selectively targeting specific tributaries or specific P forms (dissolved reactive P (DRP) vs. TP).

ELCOM-CAEDYM (Bocaniov et al., this issue) – This is a three-dimensional hydrodynamic and ecological model that dynamically couples a hydrodynamic model (Hodges et al., 2000) with a bio-geochemical model (Hipsey, 2008). The model was calibrated and applied to Lake Erie to explore the effect of mussel grazing on phytoplankton biomass, the sensitivity of thermal structure to variations in meteorological parameters, the effects of winter ice on water quality parameters, and the variability in hypoxic area extent as a function of bottom water DO concentration (Bocaniov and Scavia, in review; Bocaniov et al., 2014; Leon et al., 2011; Liu et al., 2014; Oveisy et al., 2014). As part of this application, different DO concentration thresholds (1-4 mg/L) were used for defining hypoxia when comparing P loading scenarios.

188 *Great Lakes Cladophora Model* (Auer et al., 2010; Canale and Auer, 1982; Tomlinson et al.,
189 2010) – This is a process-based model developed to understand the causes of large *Cladophora*
190 blooms in the Great Lakes (Tomlinson et al., 2010). It simulates biological processes driving
191 *Cladophora* biomass and stored P, and it predicts *Cladophora* standing crop as a function of
192 depth, light, temperature, and DRP concentration. The model was originally calibrated and
193 verified with data from Lake Huron and Lake Michigan (Tomlinson et al., 2010). For this study,
194 the model was calibrated to Lake Erie`s EB (see Scavia and DePinto, 2015) and results relating
195 *Cladophora* biomass to in-lake DRP concentrations were linked to output from the Total
196 Phosphorus Mass Balance Model and an empirical relationship between TP and DRP
197 concentrations (Chapra et al., this issue) to relate TP loads to in-lake DRP concentrations and
198 corresponding *Cladophora* biomass.

199 More recently, the *Great Lakes Cladophora* Model, was coupled with a high-resolution 3-D
200 hydrodynamic and water quality model (ELCOM-CAEDYM) to evaluate the fine-scale response
201 of *Cladophora* biomass along the northern shoreline of the EB to changes in external phosphorus
202 loads (Valipour et al., this issue). While results from this work were not available at the time the
203 original multi-model effort, they provide relevant new insight on the relative contribution of
204 local tributary loads vs. offshore-nearshore nutrient exchanges to *Cladophora* growth in the EB
205 of Lake Erie.

206 Phosphorus Loadings and Scenarios – Maccoux et al. (this issue) provides a detailed long-term
207 analysis of TP (1967-2013) and DRP (2009-2013) loads delivered annually to Lake Erie; the
208 main findings are synthesized here. The analysis confirms that after a period of gradual decline
209 in the 70s and early 80s, TP loads have shown high year-to-year variation but no clear long-term
210 trend. Inter-annual variability is largely driven by hydrometeorological conditions, which

211 modulate the timing and magnitude of surface runoff and ultimately the amount of nutrients
212 delivered to the lake (Dolan and Richards, 2008). During 2003-2013, TP from non-point sources
213 contributed on average 71% of the total annual load, while point sources accounted for 19% and
214 atmospheric load and inputs from Lake Huron made up the remaining 10%. TP loads differ
215 substantially among basins, with the WB receiving on average 60% of the whole lake load, and
216 the CB and EB receiving 28% and 12%, respectively. For 2003-2013, annual loads to the three
217 basins ranged between 487-1854 metric tons (MT) in the EB (average: 1059 MT), 1411-3703
218 MT in the CB (average: 2551 MT), and 3941-7080 MT in the WB (average: 5493 MT).

219 DRP represented on average 30% of the TP load during 2009-2013, with the WB receiving on
220 average 66% of the whole lake DRP load and the CB and EB receiving approximately 26% and
221 9%, respectively. Non-point and point sources contributed on average 49% and 39% of the total
222 annual DRP load, respectively, with atmospheric sources and loads from Lake Huron making up
223 the remaining 12%.

224 The large TP and DRP loads delivered to the WB derive overwhelmingly from two major
225 sources: the Maumee and Detroit rivers. The vast majority of the P delivered by the Maumee
226 River originates from agricultural sources (Han et al., 2012), which dominate the watershed, and
227 are the primary cause of the extremely high TP concentrations in the Maumee (and other WB
228 tributaries) compared to the Detroit River (Fig. 1). As shown in Fig. 1, the Detroit River P
229 concentration is well below that required for producing a cyanobacteria bloom.

230 While agricultural non-point sources are also primarily responsible for high DRP concentrations
231 in the Maumee, point source contributions result in relatively large DRP loads in the Detroit
232 River as well (Maccoux et al., this issue). As a consequence, while the Maumee River
233 contributes only about 5% of the total flow into the WB, it contributes approximately 48% of the

234 TP load and 31% of the DRP load. On the other hand the Detroit River contributes 41% and
235 59% of the TP and DRP load, respectively, despite accounting for over 90% of the flow (IJC,
236 2014; Maccoux et al., this issue).

237 A recent long-term (1975-2013) analysis of the Maumee River discharge and nutrient loads
238 showed that while TP concentrations remained stable since the 1990s, DRP concentrations have
239 increased (Stow et al., 2015). However, the authors also show that both TP and DRP loads have
240 increased since the 1990s as a result of a concurrent increase in river discharge. The analysis also
241 suggests the occurrence of changes in load seasonality over the past two decades, with a gradual
242 increase in March discharge and P loads. This is especially important as both TP and DRP loads
243 tend to peak in March while typically showing relatively low values from July to October (Stow
244 et al., 2015).

245 Long-term and seasonal changes in the Maumee DRP loads have received increased attention as
246 DRP is generally assumed to be readily available to algae (e.g., Baker et al., 2014). Several algal
247 bioavailability assays conducted in the Maumee River have confirmed that while DRP is
248 virtually 100% bioavailable to algae, the other major fraction of the P load – particulate
249 phosphorus (PP) – is only partially available (DePinto et al., 1981; Young et al., 1985). Results
250 from algal assays were generally consistent with chemical fractionation studies in indicating that
251 approximately 20-40% of the Maumee PP load is bioavailable (see review in Bertani et al., this
252 issue). Wherever possible, the models included in this effort accounted for the different
253 bioavailability of DRP and PP, either by explicitly incorporating processes contributing to in-
254 lake cycling (e.g., Bocaniov et al., this issue; Rucinski et al., this issue; Verhamme et al., this
255 issue; Zhang et al., this issue) or by using the best available knowledge to provide an estimate of
256 the bioavailable fraction of the P load (Bertani et al., this issue; Stumpf et al., this issue).

257 However, the load-response curves estimated by each model are expressed in terms of TP, the
258 component currently measured by most monitoring programs and directly addressed by the
259 GLWQA Nutrient Annex. In developing loading scenarios, 2008 was chosen as a baseline year
260 because its load was closest to the original 1978 Annex 3 target of 11,000 MT. At least six load
261 scenarios, defined as 0%, 25%, 50%, 75%, 100%, and 125% of the 2008 TP load, were used to
262 build load-response curves. In some cases, DRP load reductions were also evaluated.

263 **Results and Discussion**

264 ***Load-response curves***

265 *Western Basin cyanobacteria summer biomass* - The three models used to generate HAB
266 response curves identified P load from the Maumee River as the main driver of bloom size, with
267 relatively similar critical load periods across models (mid-February-June for the Bayesian model;
268 March-July for the other two models) (Fig. 2).

269 A peak 30-day average cyanobacteria biomass threshold of 9600 MT was selected to provide an
270 illustrative comparison of the effectiveness of load reductions (Table 2). This threshold was
271 chosen because most blooms perceived as "severe" since the early 2000s had satellite-estimated
272 peak 30-day mean bloom sizes > 9600 MT (Scavia and DePinto, 2015).

273 Differences in model inputs and outputs need to be taken in consideration when comparing
274 response curves. Because the models considered somewhat different loading periods, to facilitate
275 comparisons, spring load is expressed in the response curves as average monthly load (Fig. 2). In
276 addition, the models used different methods to determine peak 30-day average cyanobacteria
277 biomass. The satellite-derived estimates of maximum 30-day average bloom size used by the
278 empirical models are calculated from consecutive 10-day composite images, which are in turn

obtained by summing the highest biomass values observed at each pixel over each 10-day period (Stumpf et al., 2012). WLEEM, on the other hand, simulates daily average basin-wide cyanobacteria biomass, from which the maximum 30-day moving average is calculated (Verhamme et al., this issue). As a result, a satellite-derived bloom size of 9600 MT corresponds to a lower WLEEM-estimated bloom size. To account for this, an adjustment was made to convert the satellite-derived threshold of 9600 MT (Fig. 2a-b) to a "WLEEM equivalent" of 7830 MT (Fig. 2c) (Verhamme et al., this issue).

The load-response curves indicate that spring Maumee River TP load reductions below 180 MT/month (Stumpf et al., this issue), 178 MT/month (Verhamme et al., this issue), and 230 MT/month (under 2008 conditions; Bertani et al., this issue) result in a mean bloom size below the example threshold. These monthly loads correspond to cumulative Maumee March-July loads of 890-1150 MT (mean ± st. dev. = 980 ± 147 MT) and to cumulative Maumee annual loads of 1679-2170 MT (mean ± st. dev. = 1849 ± 278 MT) (Table 2).

The models generally agree that both the DRP and PP fractions of the TP load need to be taken into consideration when setting HAB-related load targets and that management strategies focused only on DRP will not likely be sufficient to achieve target bloom sizes (Bertani et al., this issue; Verhamme et al., this issue). WLEEM also underscores the focus on the Maumee watershed when setting HAB-related load targets (Verhamme et al., this issue). Response curves obtained by reducing the Maumee load vs. reducing loads from all WB tributaries are very similar, indicating that load reduction from the Maumee River is far more important. Their evaluation of HAB response to Detroit River TP load reductions confirms the negligible role that the Detroit River plays in bloom formation, although loads from the Detroit River do influence

301 other ecosystem properties such as TP, DRP, and total chlorophyll levels in the WB (Verhamme
302 et al., this issue), and CB hypoxia (see next section).

303 *Basin-specific overall phytoplankton biomass* – A recent long-term analysis of the trophic state
304 of the Great Lakes showed that average summer chlorophyll-*a* concentrations in the CB and EB
305 of Lake Erie rarely exceeded 2.5 μg/L over the past three decades (Dove and Chapra, 2015),
306 indicating that further decreases in summer phytoplankton biomass in these two basins are not
307 needed (Scavia and DePinto, 2015). Load-response curves for total chlorophyll are therefore
308 only presented for the WB, the most productive of the three basins (Dove and Chapra, 2015). An
309 analysis of the basin-specific TP concentrations predicted by the Total Phosphorus Mass Balance
310 model suggested that a 40% reduction from the 2008 WB and CB loads would result in a 25-
311 30% decrease in average spring TP concentrations in each basin (Chapra et al., this issue;
312 GLWQA, 2015), thereby most likely preventing significant impacts on the basins` carrying
313 capacity and fish productivity (GLWQA, 2015; Scavia and DePinto, 2015).

314 Based on analysis of model performance, four models were judged
315 suitable for exploring the relationship between WB total phytoplankton
316 biomass and external TP loading (Fig. 3). Direct comparisons across
317 load-response curves are difficult because the models used different
318 averaging periods for reporting summer mean chlorophyll-a
319 concentrations (Scavia and DePinto, 2015). To facilitate comparisons,
320 chlorophyll concentrations from each model were converted to a percent

of the chlorophyll value estimated for the highest load. All response curves were plotted as a function of WB loads (Fig. 3) because CB and EB loads have negligible influence on phytoplankton growth in the WB. Whenever whole lake loads were used in the original model application, they were converted to corresponding WB loads based on the ratio of the 2008 WB load to the whole lake load.

These models span a broad range of modeling approaches and complexity. For example, Chapra et al. (this issue) compute chlorophyll concentrations by combining a parsimonious TP mass-balance model with a relatively simple empirical relationship between August chlorophyll and in-lake TP concentrations. On the other hand, the ELCOM-CAEDYM, EcoLE, and WLEEM models simulate several complex biophysical processes and multiple ecological drivers in addition to P concentrations when predicting chlorophyll-*a*, and their results are averaged over different summer months (June-August for ELCOM-CAEDYM and EcoLE, and July-September for WLEEM). The broad diversity in model formulation, assumptions, and level of complexity provides insight on the range of expected outcomes (Fig. 3). While no specific objective was established for WB total phytoplankton biomass, it is instructive to note that reducing loads to prevent significant HABs (Table 2) would likely reduce total phytoplankton biomass by ca. 25%.

Central Basin Hypoxia – The models used for this ERI were all calibrated and to varying extent confirmed over recent but different time periods, and are therefore good representations of the current state of the system. While most models are vertically resolved into several layers that allow for a fine-scale representation of seasonal variations in DO profiles, the 9-Box model's 2-

342 layer resolution makes comparisons difficult. For this reason, the 9-Box model was not included
343 in the composite recommendations. The hypoxia response curves from each model were plotted
344 as a function of the annual WB + CB TP loads (Fig. 4). When whole lake loads were used in the
345 original model application, they were converted to WB + CB loads based on the ratio of the 2008
346 WB + CB load to the whole lake load.

347 The response curves for August-September average hypolimnetic DO concentration (Fig. 4a)
348 show similar decreasing trends with increasing loads. Some of the differences among models,
349 especially at lower loads, could be partly attributed to the fact that the 1-D model simulates
350 horizontally-averaged DO, while the other models simulate horizontally-resolved DO
351 concentrations in the bottom layer (0.5-1.0 m for ELCOM-CAEDYM; 1.0 and 1-3 m for
352 EcoLE). Differences could also be attributed to different formulations of SOD, which becomes
353 more important at lower external loads. The 1-D model (Rucinski et al., this issue) also
354 compared two different approaches to estimate loads entering the CB from the WB. One method
355 assumed a constant net apparent TP deposition rate previously estimated for the WB, whereas
356 the alternative approach used nutrient loads from the WB to the CB as simulated by WLEEM. A
357 comparison of the respective load-response curves shows that the two methods yield similar
358 results (Fig. 4).

359 There is strong convergence among models at more typical loading rates (Fig. 4a). An example
360 hypolimnetic DO concentration threshold of 4.0 mg/L was selected to compare model
361 predictions because, while hypoxia is typically defined as DO below 2.0 mg/L, Zhou et al. (
362 2013) showed that statistically significant hypoxic areas start to occur when average bottom
363 water DO concentrations are below approximately 4 mg/L. Using that as an example target

364 threshold, model predictions suggest reducing the WB + CB load to below 2600-5100 MT (mean
365 ± st. dev. = 3840 ± 1001; Table 2).

366 The models were also used to relate loads to hypoxic area (area with DO concentration < 2
367 mg/L). ELCOM-CAEDYM estimates this metric directly through its fine-scale 3-D approach;
368 the other two models use the empirical relationship between hypoxic area and bottom-layer DO
369 concentration developed by Zhou et al. (2013). As expected, all models show that hypoxic extent
370 decreases with decreasing TP loads (Fig. 4b), and suggest that decreasing the annual WB + CB
371 TP load to 3415 – 5955 MT (mean ± st. dev. = 4600 ± 989 MT) is needed to reduce the average
372 hypoxic extent to 2000 km^2 (Fig. 4b and Table 2), a value typical of the mid-1990s that coincides
373 with a period of recovery of several recreational and commercial fisheries in Lake Erie's WB
374 and CB (Ludsin et al., 2001; Scavia et al., 2014).

375 The models also estimated the influence of load reductions on the number of hypoxic days
376 (number of days when average bottom water DO is < 2 mg/L) (Fig. 4c). The models indicate that
377 a WB + CB TP load below 3415-5955 MT/year would result in a decrease in the number of
378 hypoxic days to between 9 and 42 (Fig. 4c).

379 The 1-D model simulated hypoxia response to load reductions under the broad range of
380 meteorological conditions observed between 1987 and 2005 (Rucinski et al., this issue). Results
381 indicate that the response to load reductions may show substantial inter-annual variability due to
382 meteorological forces driving mixing regimes. These findings are especially relevant in view of
383 projected changes in future climate conditions, which could result in substantial deviations in the
384 lake`s behavior from average model predictions. This uncertainty calls for an adaptive
385 management approach, where the system`s response to load reductions is assessed over time and
386 new knowledge is used to regularly update models and management strategies. Rucinski et al. (

387 this issue, 2014) also showed that variations in the lake's thermal structure produced far more
388 inter-annual variability in hypoxic area than variations in the timing, or seasonality, of the load.

389 *Eastern Basin Cladophora* – For this ERI, the Great Lakes *Cladophora* Model (Canale and Auer,
390 1982; Tomlinson et al., 2010) met the criteria required for inclusion in this effort. As described
391 in Appendix B of Scavia and DePinto (2015), several models were used to establish a
392 quantitative relationship between TP loads and *Cladophora* standing crop. The *Cladophora*
393 model was used to relate algal biomass to DRP concentrations in the EB. An empirical
394 relationship developed for the EB (Dove and Chapra, 2015) was used to relate DRP to TP
395 concentrations. Finally, the Total Phosphorus Mass Balance Model (Chapra et al., this issue) was
396 used to relate TP concentrations to external TP loads. The resulting *Cladophora* biomass-TP
397 load-response curve is shown in Fig. 5. Since there is currently no regulatory guidance on
398 acceptable levels of *Cladophora* biomass, a biomass of 30 g dry weight (DW)/m^2 was suggested
399 as a threshold likely to prevent nuisance conditions (Scavia and DePinto, 2015).

400 Model results indicate that a DRP concentration of 0.9 µg P/L (corresponding statistically to a
401 TP concentration of 6.3 µg P/L) is needed to keep *Cladophora* biomass below 30 g DW/m^2
402 (Scavia and DePinto, 2015). A whole lake TP load below 7000 MT/Year is predicted to keep TP
403 concentration below 6.3 µg P/L (Fig. 5). It is important to note that this combined modeling
404 approach was used because of time, resource, and data limitations and it is not site-specific, but
405 rather relates *Cladophora* biomass along the entire north shoreline of the EB to average offshore
406 nutrient concentrations. However, *Cladophora* proliferates in the nearshore, where it is often
407 subjected to direct impacts of point-source and tributary inputs. Nutrient concentrations in the
408 nearshore waters may therefore be higher and more variable than those in the offshore, and as

offshore DRP concentrations are reduced, control of *Cladophora* growth is expected to shift toward nearshore inputs, requiring spatially explicit models.

Some of these limitations were recently addressed (Valipour et al., this issue). Their 3-D model simulated the predominant physical processes within the *Cladophora* habitat zone (0–8 m depth) in the EB of Lake Erie, with a focus on the northern where *Cladophora* is typically most abundant. Model output was input to the *Cladophora* model to relate nearshore *Cladophora* biomass to external phosphorus loads. Results showed that while P load reductions can be expected to reduce *Cladophora* biomass in the EB, achieving proposed biomass thresholds may be more challenging than previously thought. Coastal upwelling events often input significant nutrients along much of the north shore, particularly during May and June when conditions are optimal for *Cladophora* growth. Simulations confirmed that P supplies from both the offshore and local sources (e.g. the Grand River) are capable of generating biomass above the proposed threshold. The relative importance of offshore-nearshore nutrient exchanges vs. local tributary inputs in driving nearshore P concentrations and *Cladophora* growth varies within and across years, most likely resulting in substantial variability in *Cladophora* response as whole lake loads are reduced. Generally, these results indicate that measures aimed at decreasing *Cladophora* biomass in the EB of Lake Erie should take into account nutrient sources from both the offshore region and local tributary inputs (Valipour et al., this issue).

Benefits of the multi-model approach and future research needs

Although the models vary substantially in formulations, assumptions, and parameterizations, the load-response curves generally showed considerable agreement, providing confidence in the

431 robustness of the recommendations. However, quantifying each model's uncertainty explicitly
432 would have further enhanced confidence (Kim et al., 2014). While such quantification is easily
433 accommodated in some models, it is much more difficult, if even possible, for others. The HAB
434 models provide an example. They range from a parsimonious empirical Bayesian hierarchical
435 model capable of accounting quantitatively for model error, bloom measurement error, and
436 uncertainty in parameter estimates to a complex process-based deterministic model that provides
437 model uncertainty in terms of quantitative comparisons of simulations and field observations for
438 all years simulated, but is too complex and runtime consuming for a full Monte Carlo uncertainty
439 analysis. While this illustrates a trade-off between providing causal understanding of ecosystem
440 behavior and rigorously quantifying uncertainty, it also highlights one of the benefits of the
441 multi-model approach. In that approach, the range of predicted outcomes illustrates the degree
442 of confidence in our understanding of, and the predictability of, the system's response to loads.

443 The thorough representation of uncertainty possible with the statistical models also helps identify
444 key scientific gaps limiting our predictive understanding of the system`s behavior and can guide
445 future experimental and monitoring efforts. For example, including multiple independent sets of
446 bloom observations in the Bayesian model suggests that uncertainty associated with bloom
447 characterization represents a considerable portion of overall HAB predictive uncertainty (Bertani
448 et al., this issue). More generally, the relatively large uncertainty in HAB predictions highlights
449 once again the need for adaptive management approaches that track the effectiveness of actions
450 and routinely revise models and management decisions based on new information – a point also
451 emphasized in the analysis of variability associated with meteorology in the 1D hypoxia model
452 (Rucinski et al., this issue).

In the case of hypoxia, a key source of uncertainty is quantifying the impact of changes in external loads on SOD. Previous studies have shown that SOD represents a substantial portion of total hypolimnetic oxygen demand in the CB (Rucinski et al., 2014), and both SOD and water column oxygen demand are affected by external loads. The hypoxia models used similar approaches to approximate the potential effects of changes in nutrient loads on future SOD. Rucinski et al. (this issue) coupled a relationship between SOD and organic carbon sedimentation rates (Borsuk et al., 2001) with a relationship between P loading and carbon settling from his model to predict future SOD as a function of P loads (Rucinski et al., 2014). Bocaniov et al. (this issue) and Zhang et al. (this issue) used the relationship developed by Rucinski et al. (2014), but allowed for adjustments to temperature and bottom water DO concentrations. These approaches represent our best available estimates of how SOD rates may change as a function of nutrient loads. However, future research should focus on developing long-term measurement and modeling approaches that can improve our understanding of how SOD and benthic nutrient fluxes will change as a result of external load reductions and how accumulation of nutrients and organic matter in the sediments may delay the system`s response to load reductions.

Valuable insight on critical research gaps can also be gained by exploring discrepancies among the models. For example, comparison of the HAB models suggests that quantifying the contribution of the PP component of the TP load in fueling HABs remains a critical challenge. Numerous studies have quantified the algal availability of PP in the Maumee River (see review in Bertani et al., this issue; DePinto et al., 1981; Young et al., 1985), and this knowledge has been incorporated in all three HAB models through various approaches. However, we still have limited observational knowledge of the ultimate fate of PP as it is delivered to the lake and

476 undergoes processes that influence its bioavailability, including settling, re-suspension, microbial
477 mineralization, and re-cycling by dreissenid mussels and other organisms. Stumpf et al. (this
478 issue) explicitly account for the proportion of the Maumee PP load that is assumed to settle out
479 of the water column before reaching the WB open waters based on a recent field study (Baker et
480 al., 2014b). However, field studies exploring nutrient transport dynamics along the river-lake
481 continuum in western Lake Erie are sparse, and more research is needed to quantify physical
482 processes controlling the ultimate fate of riverine nutrients. The 3-D mechanistic models (e.g.,
483 Bocaniov et al., this issue; Verhamme et al., this issue; Zhang et al., this issue) attempt to
484 explicitly characterize nutrient transport, in-lake dynamics of bioavailable P and kinetic
485 conversions among P forms (e.g., mineralization of organic P to orthophosphate, gradient-driven
486 desorption of orthophosphate from inorganic PP). However, additional measurements of *in situ*
487 biophysical processes in both the water column and sediments that can further constrain the
488 models will help reduce uncertainties.

489 Integrating results from different modeling approaches also allows for exploring processes
490 occurring at different spatio-temporal scales. For example, while the process-based HAB model
491 provides key insight into fine scale bloom spatio-temporal dynamics and underlying
492 mechanisms, the empirical models allow for assessment of system responses at longer time
493 scales. For example, the Bayesian model includes a temporal component that suggests increased
494 susceptibility of western Lake Erie to bloom formation over time, suggesting the same TP load is
495 predicted to trigger a larger bloom under present-day conditions compared to earlier years (Fig.
496 2b). Specifically, the model predicts that under 2008 lake conditions, March-June Maumee TP
497 loads below 230 MT/mo will prevent severe blooms, while under 2014 conditions a TP load of
498 230 MT/month would still result in an average bloom size of 28,000 MT (95% predictive

499 interval: 17,000-38,000 MT) (Fig. 2b). This temporal trend term, estimated by the Bayesian
500 model, remains significantly positive even after accounting for concurrent increases in DRP
501 loads, suggesting that the observed increase in DRP load alone may not be sufficient to explain
502 the apparent enhanced susceptibility. However, results from the other empirical model do not
503 support these findings. They suggest that removing the influence of the July load for relatively
504 cold years prevents under prediction of some of the most recent blooms (Stumpf et al., this
505 issue). Further research is needed to assess whether the lake is becoming more susceptible to
506 bloom formation and, if so, to identify underlying mechanisms, including the role of changes in
507 frequency, magnitude, and timing of extreme weather events (Michalak et al., 2013), the
508 potential impact of selective grazing and nutrient excretion by dreissenid mussels (Arnott and
509 Vanni, 1996; Conroy et al., 2005; Jiang et al., 2015; Vanderploeg et al., 2001; Zhang et al.,
510 2011), the influence of internal loading of both nutrients and cyanobacteria cell inocula (Chaffin
511 et al., 2014b; Rinta-Kanto et al., 2009), the role of nitrogen co-limitation (Chaffin et al., 2014a,
512 2013; Harke et al., 2015), and the influence of changes in the proportion of available vs. non-
513 available fractions of the TP load (Baker et al., 2014a; Kane et al., 2014).
514
515 **Conclusions**
516 The load-response curves presented herein represent our current best estimates of how Lake
517 Erie's ERI metrics will respond to changes in P loads, with the loadings necessary to achieve the
518 example thresholds summarized in Table 2. Results of this multi-model approach suggest:
519 • Achieving Western Basin cyanobacteria biomass reduction requires a focus on reducing
520 TP loading from the Maumee River, with an emphasis on high-flow events during March

521 - July. Results suggest that focusing on Maumee DRP load alone will not be sufficient
522 and that P load from the Detroit River is not a driver of cyanobacteria blooms.

523 • Reducing Central Basin hypoxia requires a Central + Western Basin annual load
524 reduction greater than what is needed to reach the Western Basin cyanobacteria biomass
525 goal. Load reductions focused on dissolved oxygen concentration and hypoxic areal
526 extent also result in shorter hypoxia duration.

527 • The whole lake load for achieving the proposed *Cladophora* threshold is higher than that
528 required for the hypoxia and cyanobacteria thresholds.

529 These results offered several strategies for setting loading targets under the GLWQA. The
530 thresholds in Table 2 were intended to illustrate the range of load reductions likely needed. They
531 were used by the Objectives and Targets Task Team in their recommendations to the GLWQA
532 Nutrient Annex Subcommittee on loading targets (GLWQA, 2015). Their recommendations, in
533 the context of our findings, were:

534 • *Western Basin Cyanobacteria* - To keep blooms below 9600 MT algal dry weight (the
535 size of the blooms observed in 2004 or 2012) 90% of the time, the Task Team
536 recommended a Maumee River March-July TP load of 860 MT and a DRP load of 186
537 MT, consistent with our findings. These loads represent roughly 40% reductions from the
538 2008 spring loads and correspond to Flow Weighted Mean Concentrations (FWMC) of
539 0.23 mg/L TP and 0.05 mg/L DRP. FWMC was included in the Task Team
540 recommendation to address significant inter-annual variability in Maumee River
541 discharge. It is expected that maintaining those concentrations will result in loads below
542 the targets 90% of the time, if climate change does not alter precipitation patterns. It was

543 also noted that, while reducing DRP will have a greater impact than reducing PP,
544 reducing DRP alone will not be sufficient. The Task Team also recommended 40%
545 reductions for all other WB tributaries and the Thames River.

546 • *Central Basin Hypoxia* - Our analysis suggested that setting a minimum summer average
547 hypolimnetic DO concentration of 4 mg/L or reducing hypoxia area to less than 2000 km^2
548 requires average WB + CB loads of 3840 MT and 4600 MT, respectively (Table 2). The
549 Task Team believed the load reduction to keep summer hypolimnetic DO concentrations
550 at or above 4 mg/L was so restrictive that it might reduce overall productivity and impact
551 fisheries, so they recommended an annual WB + CB TP loading target of 6000 MT,
552 closer to our area-reduction example and expected to maintain summer hypolimnion DO
553 concentrations above 2 mg/L. This load represents a 40% reduction from 2008 WB + CB
554 load levels.

555 • *Eastern Basin Cladophora* - While our analysis suggests that the cyanobacteria- and
556 hypoxia-driven load targets are sufficient to achieve a desired reduction in *Cladophora* in
557 the EB, the Task Team was not sufficiently confident in the cascade of models used to set
558 a loading target for *Cladophora*. They pointed to the need to develop a site-specific
559 model for the north shore of the EB that accounts for nutrient exchanges with the open
560 water, load and transport of specific tributaries, and the role of dreissenids to gain more
561 confidence. A spatially-explicit modeling effort was recently developed to address some
562 of these issues (Valipour et al., this issue). This work indicates that reducing nearshore
563 *Cladophora* biomass may be more challenging than previously thought, and more
564 research is needed to develop sound recommendations to address *Cladophora* growth in
565 Lake Erie.

Acknowledgments

This work was funded in part by the USEPA under contract EP-R5-11-07, Task Order 21 and by the University of Michigan Graham Sustainability Institute.

References

Arnott, D.L., Vanni, M.J., 1996. Nitrogen and phosphorus recycling by the zebra mussel (Dreissena polymorpha) in the western basin of Lake Erie. Can. J. Fish. Aquat. Sci. 53, 646–659.

Auer, M., Tomlinson, L., Higgins, S., Malkin, S., Howell, E., Bootsma, H., 2010. Great Lakes Cladophora in the 21st century: Same alga - different ecosystem. J. Great Lakes Res. 36, 248–255.

Baker, D.B., Confesor, R.B., Ewing, D.E., Johnson, L.T., Kramer, J.W., Merryfield, B.J., 2014a. Phosphorus loading to Lake Erie from the Maumee, Sandusky and Cuyahoga rivers: The importance of bioavailability. J. Great Lakes Res. 40, 502–517.

Baker, D.B., Ewing, D.E., Johnson, L.T., Kramer, J.W., Merryfield, B.J., Confesor, R.B., Richards, R.P., Roerdink, A.A., 2014b. Lagrangian analysis of the transport and processing of agricultural runoff in the lower Maumee River and Maumee Bay. J. Great Lakes Res. 40, 479–495.

Bertani, I., Obenour, D.R., Steger, C.E., Stow, C.A., Gronewold, A.D., Scavia, D., n.d. Probabilistically assessing the role of nutrient loading in harmful algal bloom formation in western Lake Erie. J. Gt. Lakes Res. This issue.

Bierman, V., 1980. A Comparison of Models Developed for Phosphorus Management in the Great Lakes, in: Conference on Phosphorus Management Strategies for the Great Lakes. pp. 1–38.

Bierman, V., Scavia, D., 2013. Hypoxia in the Gulf of Mexico: Benefits and Challenges of Using Multiple Models to Inform Management Decisions, in: Presentation at Multiple Models for Management (M3.2) in the Chesapeake Bay. Annapolis, MD.

Bierman, V.J., Dolan, D.M., 1981. Modeling of Phytoplankton-Nutrient Dynamics in Saginaw Bay, Lake Huron. J. Great Lakes Res. 7, 409–439. doi:10.1016/S0380-1330(81)72069-0

Bocaniov, S., Leon, L., Rao, Y., Schwab, D., Scavia, D., n.d. Simulating the effect of nutrient reduction on hypoxia in central Lake Erie with a three-dimensional lake model. J. Gt. Lakes Res. This issue.

Bocaniov, S., Scavia, D., n.d. Temporal and spatial dynamics of large lake hypoxia: Integrating statistical and three-dimensional dynamic models to enhance lake management criteria. Rev.

Bocaniov, S., Smith, R., Spillman, C., Hipsey, M., Leon, L., 2014. The nearshore shunt and the decline of the phytoplankton spring bloom in the Laurentian Great Lakes: Insights from a three-dimensional lake model. Hydrobiologia 731, 151–172.

605 Borsuk, M., Higdon, D., Stow, C., Reckhow, K., 2001. A Bayesian hierarchical model to predict
606 benthic oxygen demand from organic matter loading in estuaries and coastal zones. Ecol.
607 Modell. 143, 165–181.

608 Canale, R., Auer, M., 1982. Ecological studies and mathematical modeling of Cladophora in
609 Lake Huron: 5. Model development and calibration. J. Great Lakes Res. 8, 112–125.

610 Chaffin, J.D., Bridgeman, T.B., Bade, D.L., 2013. Nitrogen Constrains the Growth of Late
611 Summer Cyanobacterial Blooms in Lake Erie. Adv. Microbiol. 16–26.

612 Chaffin, J.D., Bridgeman, T.B., Bade, D.L., Mobilian, C.N., 2014a. Summer phytoplankton
613 nutrient limitation in Maumee Bay of Lake Erie during high-flow and low-flow years. J.
614 Great Lakes Res. 40, 524–531. doi:10.1016/j.jglr.2014.04.009

615 Chaffin, J.D., Sigler, V., Bridgeman, T.B., 2014b. Connecting the blooms: Tracking and
616 establishing the origin of the record-breaking Lake Erie Microcystis bloom of 2011 using
617 DGGE. Aquat. Microb. Ecol. 73, 29–39. doi:10.3354/ame01708

618 Chapra, S., Dolan, D., Dove, A., n.d. Mass-balance modeling framework for simulating and
619 managing long-term water quality for the lower Great Lakes. J. Gt. Lakes Res. This issue.

620 Chapra, S.C., Dolan, D.M., 2012. Great Lakes total phosphorus revisited: 2. Mass balance
621 modeling. J. Great Lakes Res. 38, 741–754. doi:10.1016/j.jglr.2012.10.002

622 Conroy, J.D., Edwards, W.J., Pontius, R.A., Kane, D.D., Zhang, H., Shea, J.F., Richey, J.N.,
623 Culver, D.A., 2005. Soluble nitrogen and phosphorus excretion of exotic freshwater mussels
624 (Dreissena spp.): potential impacts for nutrient remineralisation in western Lake Erie.
625 Freshw. Biol. 50, 1146–1162.

626 DePinto, J.V., Lam, D., Auer, M.T., Burns, N., Chapra, S.C., Charlton, M.N., Dolan, D.M.,
627 Kreis, R., Howell, T., Scavia, D., 2006. Examination of the status of the goals of Annex 3 of
628 the Great Lakes Water Quality Agreement.

629 DePinto, J. V., Young, T.C., Martin, S.C., 1981. Algal-Available Phosphorus in Suspended
630 Sediments from Lower Great Lakes Tributaries. J. Great Lakes Res. 7, 311–325.

631 Di Toro, D.M., Connolly, J.P., 1980. Mathematical models of water quality in large lakes. Part 2:
632 Lake Erie. EPA-600/3-80-065 Report, Duluth, MN.

633 Di Toro, D.M., Thomas, N.A., Herdendorf, C.E., Winfield, R.P., Connolly, J.P., 1987. A post
634 audit of a Lake Erie eutrophication model. J. Great Lakes Res. 13, 801–825.

635 Dolan, D., Richards, R., 2008. Analysis of late 90s phosphorus loading pulse to Lake Erie, in:
636 Munawar, M., Heath, R. (Eds.), Checking the Pulse of Lake Erie. Aquatic Ecosystem
637 Health and Management Society, Burlington, Ontario, pp. 79–96.

638 Dove, A., Chapra, S.C., 2015. Long-term trends of nutrients and trophic response variables for
639 the Great Lakes. Limnol. Oceanogr. 60, 696–721. doi:10.1002/lno.10055

640 Evans, M.A., Fahnenstiel, G., Scavia, D., 2011. Incidental oligotrophication of North American
641 Great Lakes. Environ. Sci. Technol. 45, 3297–3303. doi:10.1021/es103892w

642 GLWQA, 2015. Recommended Phosphorus Loading Targets for Lake Erie - Annex 4 Objectives
643 and Targets Task Team Final Report to the Nutrients Annex Subcommittee.

644 GLWQA, 2012. The 2012 Great Lakes Water Quality Agreement - Annex 4.
645 http://tinyurl.com/gt92hrh. Viewed 25 February 2016.

646 Han, H., Allan, J., Bosch, N., 2012. Historical pattern of phosphorus loading to Lake Erie
647 watersheds. J. Great Lakes Res. 38, 289–298.

648 Harke, M.J., Davis, T.W., Watson, S.B., Gobler, C.J., 2015. Nutrient-controlled niche
649 differentiation of western Lake Erie cyanobacterial populations revealed via
650 metatranscriptomic surveys. Environ. Sci. Technol. acs.est.5b03931.
651 doi:10.1021/acs.est.5b03931

652 Hipsey, M., 2008. The CWR Computational Aquatic Ecosystem Dynamics Model CAEDYM -
653 User Manual. Centre for Water Research, Unviersity of Western Australia.

654 Hodges, B., Imberger, J., Saggio, A., Winters, K., 2000. Modeling basin-scale internal waves in
655 a stratified lake. Limnol. Oceanogr. 1603-1620.

656 IJC, 2014. A Balanced Diet for Lake Erie: Reducing Phosphorus Loadings and Harmful Algal
657 Blooms. Report of the Lake Erie Ecosystem Priority.

658 IJC, 1988. Report on Modeling the Loading Concentration Relationship for Critical Pollutants in
659 the Great Lakes. IJC Great Lakes Water Quality Board, Toxic Substances Committee, Task
660 Force on Toxic Chemical Loadings.

661 Jiang, L., Xia, M., Ludsin, S.A., Rutherford, E.S., Mason, D.M., Marin Jarrin, J., Pangle, K.L.,
662 2015. Biophysical modeling assessment of the drivers for plankton dynamics in dreissenid-
663 colonized western Lake Erie. Ecol. Modell. 308, 18–33.
664 doi:10.1016/j.ecolmodel.2015.04.004

665 Kane, D.D., Conroy, J.D., Peter Richards, R., Baker, D.B., Culver, D.A., 2014. Re-
666 eutrophication of Lake Erie: Correlations between tributary nutrient loads and
667 phytoplankton biomass. J. Great Lakes Res. 40, 496–501. doi:10.1016/j.jglr.2014.04.004

668 Kim, D.K., Zhang, W., Watson, S., Arhonditsis, G.B., 2014. A commentary on the modelling of
669 the causal linkages among nutrient loading, harmful algal blooms, and hypoxia patterns in
670 Lake Erie. J. Great Lakes Res. 40, 117–129. doi:10.1016/j.jglr.2014.02.014

671 Lam, D., Schertzer, W., Fraser, A., 1987. A post-audit anaylsis of the NWRI nine-box water
672 quality model for Lake Erie. J. Great Lakes Res. 13, 782–800.

673 Lam, D., Schertzer, W., McCrimmon, R., Charlton, M., Millard, S., 2008. Modeling phosphorus
674 and dissolved oxygen conditions pre- and post- Dreissena arrival in Lake Erie, in:
675 Munawar, M., Heath, R. (Eds.), Checking the Pulse of Lake Erie. Aquatic Ecosystem
676 Health and Management Society, Burlington, Ontario.

677 Lam, D.C.L., Schertzer, W.M., Fraser, A.S., 1983. Simulation of Lake Erie water quality
678 responses to loading and weather variations. Environment Canada, Scientific series / Inland
679 Waters Directorate; no. 134, Burlington, Ontario.

680 Leon, L.F., Smith, R.E.H., Hipsey, M.R., Bocaniov, S.A., Higgins, S.N., Hecky, R.E.,
681 Antenucci, J.P., Imberger, J.A., Guildford, S.J., 2011. Application of a 3D hydrodynamic-
682 biological model for seasonal and spatial dynamics of water quality and phytoplankton in
683 Lake Erie. J. Great Lakes Res. 37, 41–53.

684 Lesht, B.M., Fontaine, T.D., Dolan, D.M., 1991. Great Lakes Total Phosphorus Model: Post
685 Audit and Regionalized Sensitivity Analysis. J. Great Lakes Res. 17, 3–17.
686 doi:10.1016/S0380-1330(91)71337-3

687 Liu, W., Bocaniov, S.A., Lamb, K.G., Smith, R.E.H., 2014. Three dimensional modeling of the
688 effects of changes in meteorological forcing on the thermal structure of Lake Erie. J. Great
689 Lakes Res. 40, 827–840.

690 Ludsin, S., Kershner, M., Blocksom, K., Knight, R., Stein, R., 2001. Life after death in Lake
691 Erie: nutrient controls drive fish species richness, rehabilitation. Ecol. Appl. 11, 731–746.

692 Maccoux, M., Dove, A., Backus, S., Dolan, D., n.d. Total and soluble reactive phosphorus
693 loadings to Lake Erie. J. Gt. Lakes Res. This issue.

694 Michalak, A.M., Anderson, E.J., Beletsky, D., Boland, S., Bosch, N.S., Bridgeman, T.B.,
695 Chaffin, J.D., Cho, K., Confesor, R., Daloglu, I., Depinto, J., Evans, M.A., Fahnenstiel,
696 G.L., He, L., Ho, J.C., Jenkins, L., Johengen, T.H., Kuo, K.C., Laporte, E., Liu, X.,
697 McWilliams, M.R., Moore, M.R., Posselt, D.J., Richards, R.P., Scavia, D., Steiner, A.L.,
698 Verhamme, E., Wright, D.M., Zagorski, M.A., 2013. Record-setting algal bloom in Lake
699 Erie caused by agricultural and meteorological trends consistent with expected future
700 conditions. Proc. Natl. Acad. Sci. U. S. A. 110, 6448–6452.

701 Obenour, D., Gronewold, A., Stow, C.A., Scavia, D., 2014. Using a Bayesian hierarchical model
702 to improve Lake Erie cyanobacteria bloom forecasts. Water Resour. Res. 50, 7847–7860.

703 Oveisy, A., Rao, Y.R., Leon, L.F., Bocaniov, S.A., 2014. Three-dimensional winter modeling
704 and the effects of ice cover on hydrodynamics, thermal structure and water quality in Lake
705 Erie. J. Great Lakes Res. 40, 19–28.

706 Rinta-Kanto, J.M., Saxton, M.A., DeBruyn, J.M., Smith, J.L., Marvin, C.H., Krieger, K.A.,
707 Sayler, G.S., Boyer, G.L., Wilhelm, S.W., 2009. The diversity and distribution of toxigenic
708 Microcystis spp. in present day and archived pelagic and sediment samples from Lake Erie.
709 Harmful Algae 8, 385–394. doi:10.1016/j.hal.2008.08.026

710 Rucinski, D., DePinto, J., Beletsky, D., Scavia, D., n.d. Modeling hypoxia in the Central Basin of
711 Lake Erie under potential phosphorus load reduction scenarios. J. Gt. Lakes Res. This issue.

712 Rucinski, D.K., Beletsky, D., DePinto, J. V., Schwab, D.J., Scavia, D., 2010. A simple 1-
713 dimensional, climate based dissolved oxygen model for the central basin of Lake Erie. J.
714 Great Lakes Res. 36, 465–476. doi:10.1016/j.jglr.2010.06.002

715 Rucinski, D.K., DePinto, J. V., Scavia, D., Beletsky, D., 2014. Modeling Lake Erie's hypoxia
716 response to nutrient loads and physical variability. J. Great Lakes Res. 40, 151–161.
717 doi:10.1016/j.jglr.2014.02.003

718 Scavia, D., Allan, J.D., Arend, K.K., Bartell, S., Beletsky, D., Bosch, N.S., Brandt, S.B., Briland,
719 R.D., Daloğlu, I., DePinto, J. V., Dolan, D.M., Evans, M.A., Farmer, T.M., Goto, D., Han,
720 H., Höök, T.O., Knight, R., Ludsin, S.A., Mason, D., Michalak, A.M., Richards, R.P.,
721 Roberts, J.J., Rucinski, D.K., Rutherford, E., Schwab, D.J., Sesterhenn, T.M., Zhang, H.,
722 Zhou, Y., 2014. Assessing and addressing the re-eutrophication of Lake Erie: Central basin
723 hypoxia. J. Great Lakes Res. 40, 226–246.

724 Scavia, D., DePinto, J. V., 2015. Great Lakes Water Quality Agreement Nutrient Annex

725 Objectives and Targets Task Team Ensemble Modeling Report. http://tinyurl.com/ng6d3tn.
726 Viewed 25 February 2016.

727 Scavia, D., Justic, D., Bierman, V., 2004. Reducing Hypoxia in the Gulf of Mexico: Advice from
728 Three Models. Estuaries 27, 419–425.

729 Stow, C., Roessler, C., Borsuk, M., Bowen, J., Reckhow, K., 2003. Comparison of Estuarine
730 Water Quality Models for Total Maximum Daily Load Development in Neuse River
731 Estuary. J. Water Resour. Plan. Manag. 129, 307–314.

732 Stow, C.A., Cha, Y., Johnson, L.T., Confesor, R., Richards, R.P., 2015. Long-term and seasonal
733 trend decomposition of Maumee River nutrient inputs to western Lake Erie. Environ. Sci.
734 Technol. 49, 3392–400. doi:10.1021/es5062648

735 Stumpf, R., Johnson, L., Wynne, T., Baker, D., n.d. Forecasting annual cyanobacterial bloom
736 biomass to inform management decisions in Lake Erie. J. Gt. Lakes Res. This issue.

737 Stumpf, R.P., Wynne, T.T., Baker, D.B., Fahnenstiel, G.L., 2012. Interannual variability of
738 cyanobacterial blooms in Lake Erie. PLoS One 7, e42444.

739 Tomlinson, L., Auer, M., Bootsma, H., 2010. The Great Lakes Cladophora Model: Development
740 and application to Lake Michigan. J. Great Lakes Res. 36, 287–297.

741 Valipour, R., Leon, L., Depew, D., Dove, A., Rao, Y., n.d. High-resolution modeling for
742 development of nearshore ecosystem objectives in eastern Lake Erie. J. Gt. Lakes Res. This
743 issue.

744 Vallentyne, J.R., Thomas, N.A., 1978. Fifth Year Review of Canada-United State Great Lakes
745 Water Quality Agreement. Report of Task Group III. A Technical Group to Review
746 Phosphorus Loadings.

747 Vanderploeg, H.A., Liebig, J.R., Carmichael, W.W., Agy, M.A., Johengen, T.H., Fahnenstiel,
748 G.L., Nalepa, T.F., 2001. Zebra mussel (Dreissena polymorpha) selective filtration
749 promoted toxic Microcystis blooms in Saginaw Bay (Lake Huron) and Lake Erie. Can. J.
750 Fish. Aquat. Sci. 58, 1208–1221.

751 Verhamme, E., Redder, T., Schlea, D., Grush, J., Bratton, J., DePinto, J., n.d. Development of
752 the Western Lake Erie Ecosystem Model (WLEEM): application to connect phosphorus
753 loads to cyanobacteria biomass. J. Gt. Lakes Res. This issue.

754 Vollenweider, R., 1976. Advances in defining critical loading levels for phosphorus in lake
755 eutrophication. Mem. dell`Istituto Ital. di Idrobiol. 33, 53–83.

756 Weller, D.E., Benham, B., Friedrichs, M., Najjar, R., Paolisso, M., Pascual, P., Shenk, G.,
757 Sellner, K., 2013. Multiple Models for Management in the Chesapeake Bay. STAC
758 Publication Number 14-004, Edgewater, MD.

759 Young, T.C., Depinto, J. V, Martin, S.C., Bonner, J.S., 1985. Algal-Available Particulate
760 Phosphorus in the Great Lakes Basin. J. Great Lakes Res. 11, 434–446.

761 Zhang, H., Culver, D. a., Boegman, L., 2008. A two-dimensional ecological model of Lake Erie:
762 Application to estimate dreissenid impacts on large lake plankton populations. Ecol.
763 Modell. 214, 219–241. doi:10.1016/j.ecolmodel.2008.02.005

764 Zhang, H., Culver, D., Boegman, L., 2011. Dreissenids in Lake Erie: an algal filter or a
765 fertilizer? Aquat. Invasions 6, 175–194.

766 Zhang, H., Culver, D., Boegman, L., n.d. Spatial distributions of external and internal
767 phosphorus loads and their impacts on Lake Erie`s phytoplankton. J. Gt. Lakes Res. This
768 issue.

769 Zhou, Y., Obenour, D.R., Scavia, D., Johengen, T.H., Michalak, A.M., 2013. Spatial and
770 temporal trends in Lake Erie hypoxia, 1987-2007. Environ. Sci. Technol. 47, 899–905.
771 doi:10.1021/es303401b

772

Figure Captions

Figure 1. Annual average TP and DRP loads delivered to the Western Basin by major tributaries (upper panel), and annual average flow (lower left panel) and flow weighted mean TP concentration (FWMC, lower right panel) from the same tributaries.

Figure 2. WB cyanobacteria bloom size predicted by three different models as a function of spring Maumee River TP load: a) NOAA Western Lake Erie HAB model; b) U-M/GLERL Western Lake Erie HAB model; c) Western Lake Erie Ecosystem Model (WLEEM). Solid lines are mean model predictions, while dashed lines and shaded area represent 95% predictive intervals. In a), 70% predictive intervals are also shown as reported in Stumpf et al. (this issue). In b), model predictions under 2008 (grey) and 2014 (black) lake conditions are shown. Because the models consider different spring load periods (see text), Maumee River load is reported as MT/month to facilitate comparison across models. The horizontal line indicates the threshold for "severe" blooms, which equals 9600 MT for the first two models and was adjusted to an equivalent of 7830 MT for the WLEEM model (see text and Verhamme et al., this issue). The corresponding March-July cumulative loads are reported in Table 2.

Figure 3. Average summer chlorophyll–*a* concentration in the WB predicted by different models as a function of annual WB TP loads. Each response curve has been scaled to 100% at its maximum chlorophyll value to facilitate comparisons. The dashed line represents a 40% reduction from the 2008 WB annual load.

Figure 4. CB hypoxia metrics predicted by different models as a function of WB + CB annual TP load: a) August-September average hypolimnetic DO concentration in the CB. The horizontal line represents the average concentration (4 mg/L) corresponding to initiation of statistically significant hypoxic areas (Zhou et al., 2013); b) August-September average extent of the CB

hypoxic area. The horizontal line indicates a threshold of 2000 km^2; c) Number of hypoxic days in the CB. The shaded area indicates the range of loads required to achieve the hypoxic area threshold of 2000 km^2. Results for the EcoLE model are shown considering a bottom layer of 1 m (EcoLE_1m) and 1-3 m (EcoLE_1-3m). Results for the 1-D hypoxia model are shown considering a constant net apparent TP deposition rate in the WB (1D Hypoxia_WBconst) and considering TP loads from the WB to the CB as simulated by the WLEEM model (1D Hypoxia_WLEEM).

Figure 5. *Cladophora* biomass predicted by the Great Lakes *Cladophora* model (GLCM) in the EB as a function of whole lake annual TP load. The horizontal line represents an example biomass threshold of 30 g/m^2.

Table 1. Models included in the multi-model effort and Ecosystem Response Indicators (ERIs) addressed by each.

	Ecosystem Response Indicators			
	Basin-specific overall phytoplankton biomass	**WB cyanobacteria peak summer biomass**	**CB hypoxia**	**EB *Cladophora***
NOAA Western Lake Erie HAB Model		X		
U-M/GLERL Western Lake Erie HAB Model		X		
Total Phosphorus Mass Balance Model	X			
1-D Central Basin Hypoxia Model	X (CB only)		X	
Ecological Model of Lake Erie (EcoLE)	X (WB only)		X	
Nine-Box Model			X	
Western Lake Erie Ecosystem Model (WLEEM)	X (WB only)	X		
ELCOM-CAEDYM	X		X	
Great Lakes *Cladophora* Model (GLCM)				X

Table 2. TP loads (MT) associated with example ERI thresholds. Annual Maumee River TP loads corresponding to the suggested March - July loads were calculated assuming the March-July load represents on average 53% of the annual load (data from Heidelberg University`s National Center for Water Quality Research, http://tinyurl.com/zgkberb). The corresponding WB annual loads were calculated assuming the Maumee annual load represents on average 48% of the whole WB annual load (Maccoux et al., this issue).The whole lake annual loads corresponding to the suggested hypoxia-related WB+CB loads were calculated assuming the WB+CB load represents on average 88% of the whole lake load (Maccoux et al., this issue).

Model	Maumee March-July load to achieve threshold	Maumee annual load to achieve threshold	WB annual load to achieve threshold	WB + CB annual load to achieve threshold	Whole lake annual load to achieve threshold
Loads to reduce Western Basin Cyanobacteria to 9600 MT cell DW					
UM/GLERL_2008	1150	2170	4520		
NOAA	900	1698	3538		
WLEEM	890	1679	3498		
Mean ± St. Dev.	**980 ±147 ***	**1849 ± 278***	**3852 ± 579***	***using UM/GLERL_2008**	
Loads to reduce Central Basin Hypolimnetic Dissolved Oxygen to 4 mg/l					
EcoLE_1-3m				4400	5000
EcoLE_1m				2600	2955
ELCOM-CAEDYM				3100	3523
1D CB Hypoxia_WBconst				5100	5795
1D CB Hypoxia _WLEEM				4000	4545
Mean ± St. Dev.				**3840 ±1001**	**4364 ±1138**
Loads to reduce Central Basin Hypoxic Area to 2000 km^2					
EcoLE_1-3m				5955	6767
EcoLE_1m				3415	3881
ELCOM-CAEDYM				4920	5591
1D CB Hypoxia_WBconst				4830	5489
1D CB Hypoxia _WLEEM				3880	4409
Mean ± St. Dev.			*omitting 9=Box	**4600 ± 989***	**5227 ± 1124***
Loads to reduce *Cladophora* dry weight biomass to 30 g/m^2					
GLCM					7000

Figure 1. Annual average TP and DRP loads delivered to the Western Basin by major tributaries (upper panel), and annual average flow (lower left panel) and flow weighted mean TP concentration (FWMC, lower right panel) from the same tributaries.

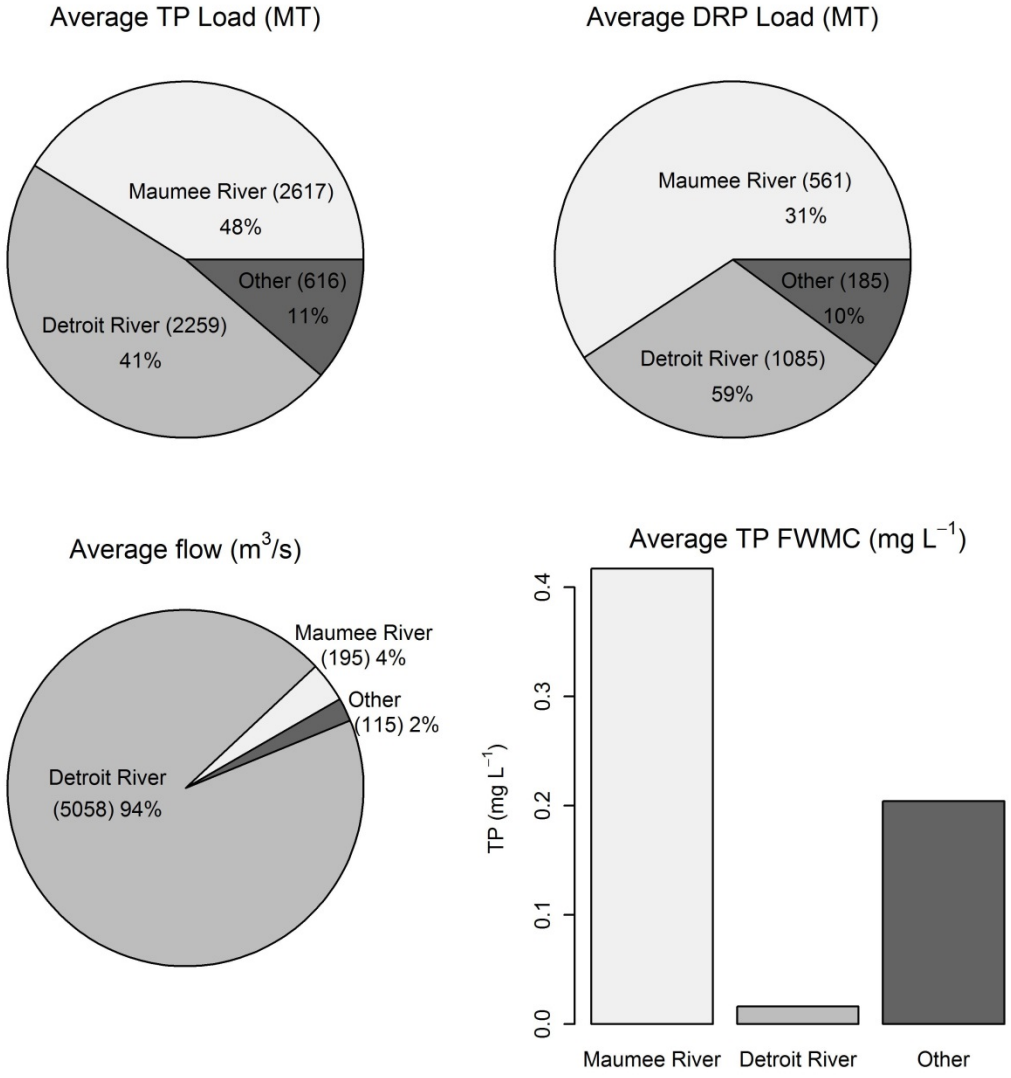

Figure 2. WB cyanobacteria bloom size predicted by three different models as a function of spring Maumee River TP load: a) NOAA Western Lake Erie HAB model; b) U-M/GLERL Western Lake Erie HAB model; c) Western Lake Erie Ecosystem Model (WLEEM). Solid lines are mean model predictions, while dashed lines and shaded area represent 95% predictive intervals. In a), 70% predictive intervals are also shown as reported in Stumpf et al. (this issue). In b), model predictions under 2008 (grey) and 2014 (black) lake conditions are shown. Because the models consider different spring load periods (see text), Maumee River load is reported as MT/month to facilitate comparison across models. The horizontal line indicates the threshold for "severe" blooms, which equals 9600 MT for the first two models and was adjusted to an equivalent of 7830 MT for the WLEEM model (see text and Verhamme et al., this issue). The corresponding March-July cumulative loads are reported in Table 2.

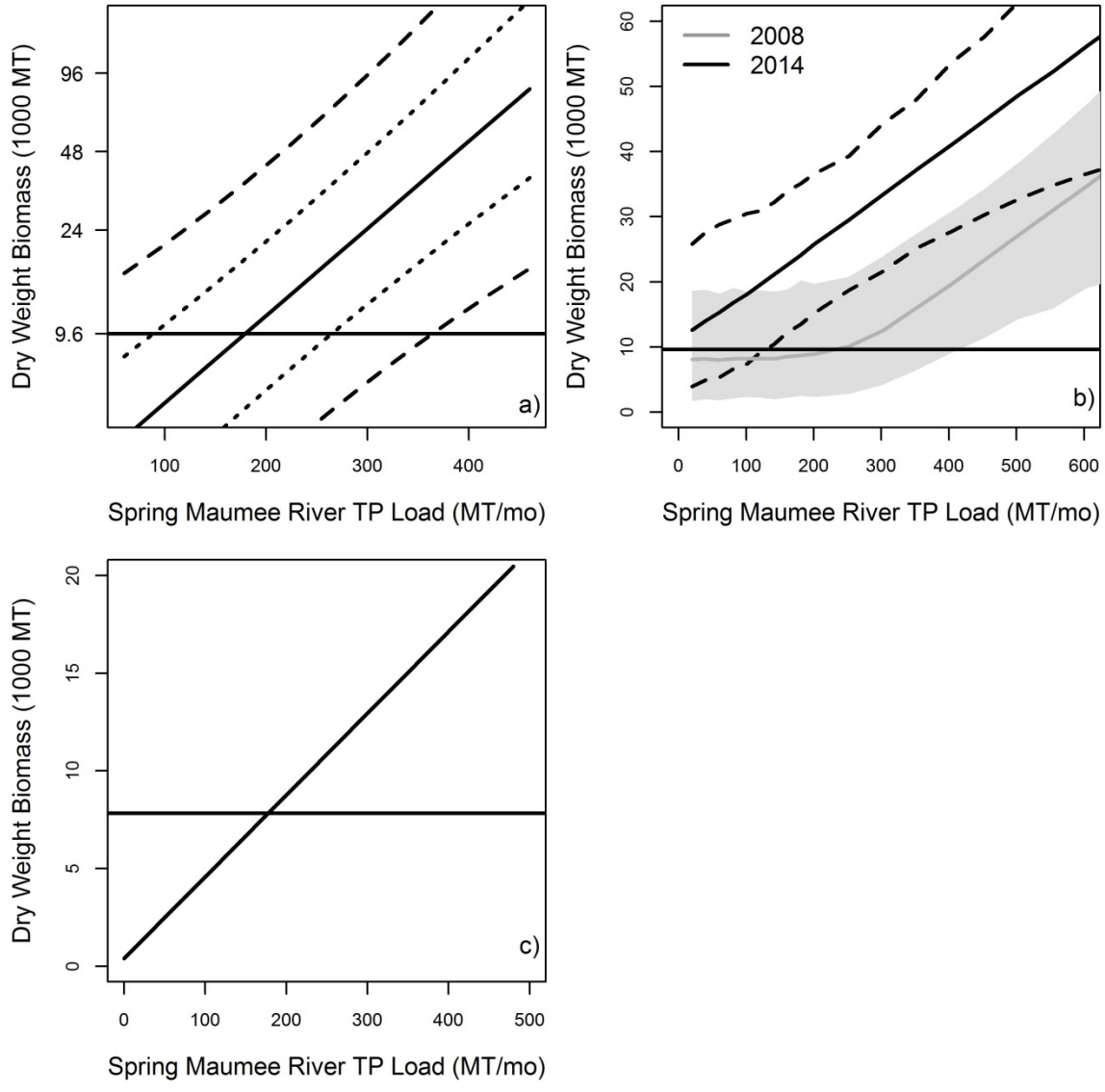

Figure 3. Average summer chlorophyll–*a* concentration in the WB predicted by different models as a function of annual WB TP loads. Each response curve has been scaled to 100% at its maximum chlorophyll value to facilitate comparisons. The dashed line represents a 40% reduction from the 2008 WB annual load.

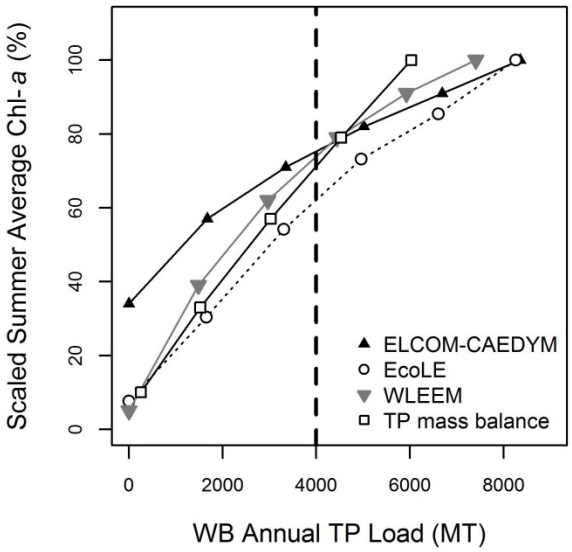

Figure 4. CB hypoxia metrics predicted by different models as a function of WB + CB annual TP load: a) August-September average hypolimnetic DO concentration in the CB. The horizontal line represents the average concentration (4 mg/L) corresponding to initiation of statistically significant hypoxic areas (Zhou et al., 2013); b) August-September average extent of the CB hypoxic area. The horizontal line indicates a threshold of 2000 km^2; c) Number of hypoxic days in the CB. The shaded area indicates the range of loads required to achieve the hypoxic area threshold of 2000 km^2. Results for the EcoLE model are shown considering a bottom layer of 1 m (EcoLE_1m) and 1-3 m (EcoLE_1-3m). Results for the 1-D hypoxia model are shown considering a constant net apparent TP deposition rate in the WB (1D Hypoxia_WBconst) and considering TP loads from the WB to the CB as simulated by the WLEEM model (1D Hypoxia_WLEEM).

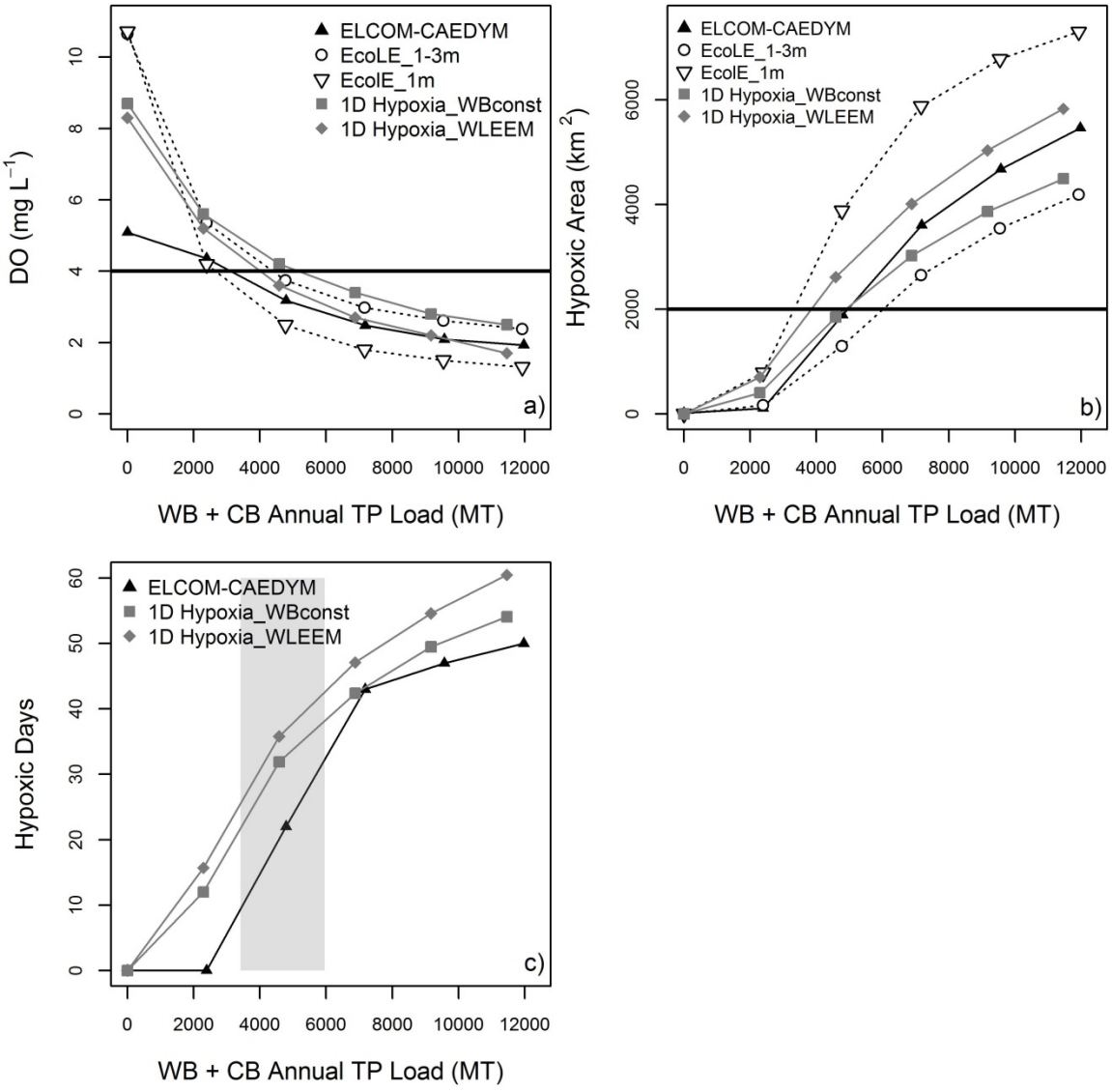

Figure 5. *Cladophora* biomass predicted by the Great Lakes *Cladophora* model (GLCM) in the EB as a function of whole lake annual TP load. The horizontal line represents an example biomass threshold of 30 g/m^2.